Front. Optoelectron. 2019, 12(4): 382–391
https://doi.org/10.1007/s12200-019-0915-4

RESEARCH ARTICLE

# Ultra-flat broadband microwave frequency comb generation based on optical frequency comb with a multiple-quantum-well electro-absorption modulator in critical state

**Cong SHEN, Peili LI (✉), Xinyuan ZHU, Yuanfang ZHANG, Yaqiao HAN**

College of Electronic and Optical Engineering, College of Microelectronics, Nanjing University of Posts and Telecommunications, Nanjing 210042, China



**Abstract** In this paper, we proposed a novel ultra-flat broadband microwave frequency comb (MFC) generation based on optical frequency comb (OFC) with a multiple-quantum-well electro-absorption modulator (MQW-EAM) in critical state. The scheme is simple and easy to adjust. The performance of the MFC generation scheme is investigated using software Optisystem. The results show that the comb spacing of MFC can be adjusted from 5 to 20 GHz by changing RF signal's frequency and the MFC is almost independent on the linewidth of the tunable laser diode. The performance of the MFC can be improved by reasonably increasing the voltage of the RF, the small-signal gain of the Erbium-doped fiber amplifier (EDFA) and the responsivity of the photodetector. The MFC generated by this scheme has 300 GHz effective bandwidth with 15 comb lines, whose power variation is 0.02 dB, when the components' parameters in the Optisystem are set as follows: the power of tunable laser diode (TLD) is 0 dBm, the wavelength is 1552.52 nm, and linewidth is 1 MHz; RF signal's frequency is 20 GHz and the voltage is 10 V; the reverse bias voltage of MQW-EAM is 6.92 V; the small-signal gain of the EDFA is 40 dB; the responsivity of the photodetector (PD) is 1 A/W.

**Keywords** microwave frequency comb (MFC), multiple-quantum-well electro-absorption modulator (MQW-EAM), flatness

## 1 Introduction

Microwave frequency comb (MFC) has potential applications in many fields such as communications, military, measurement and so on [1–5], by virtue of a large number of spectral lines, a wide frequency range, and high precision of spectral line spacing. So MFCs have attracted considerable attention.

Many schemes for generating MFCs have been proposed, which are mainly divided into two categories: electronic methods [6,7] and optical methods [8–16]. Compared to the electronic methods limited by the electronic bandwidths, the schemes for generating MFC by optical methods can generate broader-bandwidth MFC. So the optical schemes for MFC generation are topics of current research. Many optical methods have been proposed, such as focusing ultrafast laser pulse on the tunneling junction of a scanning tunneling microscope [8,9], using nonlinear dynamics of semiconductor lasers [10–12], using mode-locked laser [13,14]. These methods have their own unique advantages, but there is also room for improvement. For example, in the method based on focusing ultrafast laser pulse on the tunneling junction of a scanning tunneling microscope, the comb spacing of MFCs is determined by the repetition frequency of the pulse output from the laser and cannot be adjusted arbitrarily. In view of the scheme by using nonlinear dynamics of semiconductor lasers, the nonlinear dynamics is difficult to be adjusted to generate MFCs. As for the methods by using mode-lock laser to generate MFCs, it is not easy to adjust the laser to make it mode locked and the comb spacing of MFC cannot be adjusted arbitrarily. In addition to these methods, the schemes by utilizing external modulation [15,16] also attracted great attention, and MFCs generated have large bandwidths and great tunability. A flexibly tunable MFC is generated based on optical heterodyning between the intensity-modulated optical carrier and the frequency-shifted Stokes light, which contains 20 lines with 1 GHz comb spacing, while the power variation is larger than 25 dB [15]. Based on a

Received March 9, 2019; accepted April 29, 2019

E-mail: lipl@njupt.edu.cn

dual-output Mach-Zehnder modulator and balanced detection, the MFC generated has the bandwidth of 20 GHz and the power variation of 1.1 dB, and the comb spacing can be adjusted from 5 to 10 GHz [16]. The bandwith and flatness of MFC by utilizing external modulation still have room for improvement.

In this paper, a novel scheme for the generation of ultra-flat broadband MFC is proposed. In this scheme, the multiple-quantum-well electro-absorption modulator (MQW-EAM) [17] in critical state is used to generate an optical frequency comb (OFC), whose spectrum consists of high-power central carrier and ultra-flat, low-power sidebands. Then, the MFC is achieved by beatings of the OFC in the photodetector (PD). This scheme is simple in structure and easy to adjust, and the MFC generated by it has better comprehensive performance, such as good flatness, wide bandwith and good tunability. The performance of the generated MFC was investigated using the software Optisystem. We investigated the effects of some parameters, such as the linewidth of the tunable laser diode (TLD), the reverse bias voltage of the MQW-EAM, the voltage and frequency of the RF signal, the small-signal gain of the Erbium-doped fiber amplifier (EDFA) and the responsivity of the PD, on the performance of the generated MFC.

## 2 Operation principle

The schematic diagram of the proposed ultra-flat microwave frequency combs generation based on optical frequency comb with a MQW-EAM is shown in Fig. 1. The single-wavelength carrier provided by the TLD is input into the MQW-EAM, which is driven and modulated by a RF signal. The output optical spectrum from the modulator is an OFC with Gaussian envelope when the reverse bias voltage $V_b$ is relatively small. With the increase of the $V_b$, the envelope-peak power decreases and the bandwidth of the Gaussian envelope increases, while the power of central carrier remains almost constant. There exists a certain $V_b$, which makes MQW-EAM in critical state [18]. When MQW-EAM is in critical state, the output optical spectrum consists of the ultra-flat, low-power sidebands and the high-power central carrier. With the $V_b$ increasing further, the sidebands will decrease rapidly and disappear, while the central carrier is still reserved. With the change of the voltage of RF signal $V_{RF}$, the $V_b$ corresponding to the critical state of MQW-EAM will be also changed at the same time. So we can adjust the $V_{RF}$ and the $V_b$ to make the MQW-EAM in critical state. The output optical spectrum from MQW-EAM is input into the EDFA and amplified. Then, the amplified OFC is input into the PD to generate the electrical spectrum by beatings among sidebands and carrier, and the MFC is achieved. During the process of beatings, the high-power carrier plays a dominant role and the beating signals between any two low-power sidebands can be almost ignored, so the power variation of the MFC generated form PD can be very small.

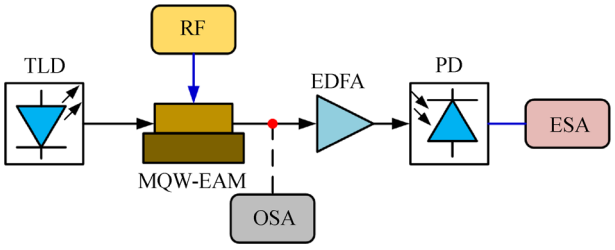


**Fig. 1** Schematic diagram of ultra-flat microwave frequency combs generation based on a single electro-absorption modulator. TLD: tunable laser diode; MQW-EAM: multi-quantum well based electro-absorption modulator; RF: radio frequency; EDFA: Erbium-doped fiber amplifier; PD: photodetector; OSA: optical spectrum analyzer; ESA: electrical spectrum analyzer

## 3 Theory model

The TLD provides a single-wavelength light as the carrier, and the electric field $E_{in}(t)$ is expressed as follows:

$$E_{in}(t) = E_0 \exp(j2\pi f_c t), \tag{1}$$

where $f_c$ denotes the input optical signal frequency; $E_0$ is the amplitude constant.

Then, the light is input into the MQW-EAM and modulated, and the output electric field from the MQW-EAM $E_{out}(t)$ can be expressed as follows [19]:

$$E_{out}(t) = E_0^{1+j\alpha} \exp\{-[V_b(1 + m\sin 2\pi f_m t)/V_0]^a (1 + j\alpha)\} \cdot \exp(j2\pi f_c t), \tag{2}$$

where $\alpha$ denotes the linewidth enhancement factor; $V_b$ represents the reverse bias voltage; $m$ is the modulation index, and $m = V_{RF}/V_b (0 \leqslant m \leqslant 1)$, where $V_{RF}$ represents the voltage of RF signal; $f_m$ represents modulation frequency; $V_0$ represents the reverse bias voltage when the output optical power is $P_0/e$, where $P_0$ denotes the power of the input light; $a$ represents a constant, which is generally 3 – 4 for MQW-EAM.

$E_{out}(t)$ is generally expressed in the following relation after Fourier transform:

$$E_{out}(t) = E_0^{1+j\alpha} \left\{ \begin{array}{l} S_{p0} \exp(j2\pi f_c t) + \frac{S_{p1}}{2} \exp[j2\pi(f_c \pm f_m)t] \\ + \frac{S_{p2}}{2} \exp[j2\pi(f_c \pm 2f_m)t] + \cdots \end{array} \right\}, \tag{3}$$

where $S_{pi} (i = 0,1,2,...)$ denotes the amplitude of the central carrier and sidebands at the output of the modulator.

When the parameter $a$ is an integer, $S_{p0}$ and $S_{p1}$ in Eq. (3) can be given by

$$S_{p0} = 1 + \sum_{p=1}^{\infty}\left[\frac{(-\gamma')^p}{p}\right] + \sum_{n=1}^{\infty}\left\{C_{2n}^{n}\frac{m^{2n}}{2^{2n}}\sum_{p=p_0}^{\infty}\left[\frac{C_{ap}^{2n}(-\gamma')^p}{p!}\right]\right\}, \quad (4)$$

$$S_{p1} = \sum_{n=1}^{\infty}\left\{C_{2n-1}^{n-1}\frac{m^{2n-1}}{2^{2n-2}}\sum_{p=p_1}^{\infty}\left[\frac{C_{ap}^{2n-1}(-\gamma')^p}{p!}\right]\right\}, \quad (5)$$

where $\gamma' = (1+\mathrm{j}\alpha)(V_b^a/2V_0^a)$; $p_0$ and $p_1$ are integers and dependent on $a$.

As can be seen from Eqs. (3)–(5), the output optical spectrum has $2i+1$ comb lines, and the power of the carrier and sidebands is dependent on $V_\mathrm{b}$, $V_\mathrm{RF}$ and $V_0$. We can adjust the parameters to make the MQW-EAM in critical state, where the power of central carrier is higher a lot than that of sidebands and the power variation of sidebands is very small. The relation can be given by

$$S_{p0} >> S_{pi}(i \neq 0) \quad \text{and} \quad S_{p1} \approx S_{p2} \approx S_{p3} \cdots \approx S_{pi}(i \neq 0). \quad (6)$$

Then, the output optical spectrum is amplified by the EDFA and input into the PD to generate the MFC by beatings among sidebands and carrier. The generation photocurrent at the output of the PD can be given by [20]

$$\begin{aligned} i(t) \propto & \left(S_{p0}^2 + \frac{1}{2}(S_{p1}^2 + S_{p2}^2 + S_{p3}^2 + S_{p4}^2 + \cdots + S_{pn}^2)\right) + \left(S_{p0}S_{p1} + \frac{1}{2}\left(S_{p1}S_{p2} + \cdots + S_{p(n-1)}S_{pn}\right)\right)\cos(\omega_m t) \\ & + \left(S_{p0}S_{p2} + \frac{1}{2}\left(S_{p1}S_{p3} + \cdots + S_{p(n-2)}S_{pn} + S_{p1}^2\right)\right)\cos(2\omega_m t) \\ & + \left(S_{p0}S_{p3} + \frac{1}{2}\left(S_{p1}S_{p4} + \cdots + S_{p(n-3)}S_{pn} + S_{p1}S_{p2}\right)\right)\cos(3\omega_m t) \\ & + \cdots \\ & + \left(S_{p0}S_{pn} + \frac{1}{4}\sum_{k=1}^{n-1}\left(S_{pk}S_{p(n-k)}\right)\right)\cos(n\omega_m t) + \frac{1}{4}\sum_{h=n+1}^{2n}\sum_{k=1}^{h-1}\left(S_{pk}S_{p(h-k)}\right)\cos(h\omega_m t). \end{aligned} \quad (7)$$

As can be seen from Eq. (7), each frequency of the MFC is obtained by adding multiple items. While, $S_{p0}$ is much larger than $S_{pi}$ ($i \neq 0$), so the term containing $S_{p0}$ dominates the amplitude of each frequency. Therefore, the MFC can also been seen as beatings between the central carrier and each sideband, and other beating signals between any two sidebands can be almost ignored. Smaller the power variation of optical sidebands is, flatter the MFC is. So adjusting $V_\mathrm{b}$ and $V_\mathrm{RF}$ to make the MQW-EAM in critical state is the key to our scheme.

## 4 Simulation results and discussion

The proposed scheme for ultra-flat broadband microwave frequency combs generation based on a single electro-absorption modulator is simulated by using the software Optisystem. The components' parameters in the system are set as follows: TLD's power is 0 dBm, optical wavelength $\lambda$ is 1552.52 nm, and linewidth is 1 MHz; RF signal's frequency is 20 GHz and the voltage $V_\mathrm{RF}$ is 10 V; the reverse bias voltage $V_\mathrm{b}$ of MQW-EAM is 6.92 V; the Er ion density of Erbium-doped fiber is $10^{25}/\mathrm{m}^3$, the length is 6 m, the forward pump power is 275 mW and the small-signal gain of the EDFA is 40 dB; the responsivity of the PD is 1 A/W, the dark current is 10 nA. All parameters of the components remain unchanged unless noted otherwise.

Figure 2 shows the output optical spectrum from MQW-EAM and the corresponding output electrical spectrum from PD. As can be seen from Fig. 2(a), the output optical spectrum from the MQW-EAM is a 32-line OFC, where the power of the carrier is −20.07 dBm and the average power of the sidebands is −51.18 dBm with the power variation of 0.04 dB. As can be seen from Fig. 2(b), the corresponding output electrical spectrum from PD has the power variation of 0.02 dB with 15 comb lines, the average power is −29.86 dB and the effective bandwidth is 300 GHz.

### 4.1 Effects of the reverse bias voltage

Figure 3 shows the output optical spectra from the MQW-EAM and the corresponding output electrical spectra from the PD when the reverse bias voltage $V_\mathrm{b}$ is 6.52, 6.72, 6.92 and 7.12 V, respectively. When the $V_\mathrm{b}$ is relatively small, for example $V_\mathrm{b}$ is 6.52 V, the output optical spectrum is an OFC consisting of the carrier and the sidebands of Gaussian envelope. As can be seen from Fig. 3(a), the OFC has Gaussian-envelope sidebands with the power variation of 26.91 dB when the $V_\mathrm{b}$ is 6.52 V. The output

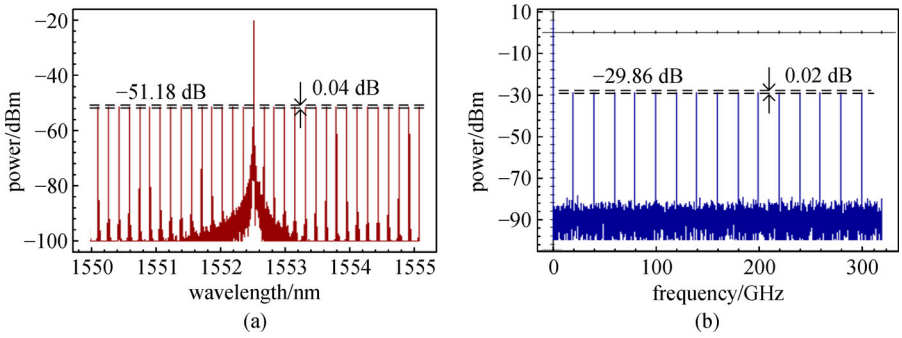


**Fig. 2** (a) Output optical spectrum from MQW-EAM; (b) corresponding output electrical spectrum from PD

corresponding electrical spectrum has the power variation of 56.51 dB as shown in Fig. 3(e). When the $V_b$ is increased, the envelope-peak power decreases and the bandwidth of the Gaussian envelope increases, while the power of the carrier remains almost constant. As can be seen from Figs. 3(a) and 3(b), the power variation of the sidebands is improved from 26.91 to 23.93 dB when the $V_b$ is increased from 6.52 to 6.72 V and the power variation of the corresponding electrical spectrum is also improved from 56.51 to 45.36 dB as shown in Figs. 3(e) and 3(f). When $V_b$ is increased to 6.92 V, the MQW-EAM is in critical state. The output optical spectrum consists of ultra-flat, low-power sidebands and high-power central carrier as shown in Fig. 3(c). The average power of the sidebands with the power variation of 0.04 dB is −51.18 dBm and the power of the carrier is −20.07 dBm. The corresponding MFC generated by beatings is very flat, whose power variation is 0.02 dB, as shown in Fig. 3(g). The reason is that the high-power carrier plays a dominant role and the sidebands are ultra-flat at the same time. With the $V_b$ increased further to 7.12 V, the sidebands will decrease rapidly and disappear, while the central carrier is still reserved, as shown in Fig. 3(d). Deservedly, the microwave signal disappears as shown in Fig. 3(h).

### 4.2 Effects of the voltage of RF

The reserve bias voltage $V_b$ corresponding to the critical state of MQW-EAM will change along with the change of the voltage of RF signal $V_{RF}$. When the $V_{RF}$ changes, the $V_b$ should be adjusted to ensure the MQW-EAM in critical state. Figure 4 shows the spectra of the MFC when the $V_{RF}$ is 1, 4, 7 and 10 V, and the corresponding $V_b$ is 2.49, 3.97, 5.43 and 6.92 V to make the MQW-EAM in critical state respectively. As can be seen that, the average power of the MFC becomes higher along with the increase of the $V_{RF}$. Besides, the power variation of the MFC also decreases from 0.11 to 0.02 dB with the increase of the $V_{RF}$. So the performance of the MFC can be improved by increasing the $V_{RF}$.

### 4.3 Effects of the frequency of RF

The reserve bias voltage $V_b$ corresponding to the critical state of MQW-EAM will change along with the change of the frequency of RF signal. When the frequency of RF signal changes, the $V_b$ should be adjusted to ensure the MQW-EAM in critical state. Figure 5 shows the spectra of the MFC when the frequency of RF signal is 5, 10, 15 and 20 GHz, and the corresponding $V_b$ is 6.99, 6.98, 6.97 and 6.92 V to make the MQW-EAM in critical state respectively. As can be seen that, the comb spacing of MFC is 5, 10, 15 and 20 GHz, respectively, which is equal to the frequency of RF signal. Besides, with the increase of RF signal's frequency, the average power of the MFC becomes higher and the power variation decreases from 2.12 to 0.02 dB. The reason is that, the lower the frequency of RF signal, the larger the $V_b$ corresponding to the critical state is. The absorption of light by MQW-EAM will become larger with the increase of $V_b$ , and the transmitted light power decreases, so the average power of MFC generated by beating decreases at the same time. And low-power MFC is more susceptible to noise, so the power variation is larger when the frequency of RF signal is low. Therefore, the comb spacing of MFC can be adjusted from 5 to 20 GHz by changing RF signal's frequency, and the average power of MFC is larger and the power variation is less when the RF signal's frequency is higher.

### 4.4 Effects of the fluctuation of the voltages

In real experiments, the adjustment of $V_b$ or $V_{RF}$ may not necessarily make MQW-EAM exactly in the critical state, and there may be a certain deviation from the ideal value. So we take the fluctuation of the $V_b$ as an example to study the effects of the voltage deviation on the MFC. Figure 6 shows the output electrical spectra from the PD when the voltage of RF signal $V_{RF}$ is 10 V and the reverse bias voltage $V_b$ is 6.90, 6.91, 6.92 and 6.93 V, respectively. We can see that the corresponding average power is −27.51, −28.66, −29.86 and −31.19 dBm, which decreases along

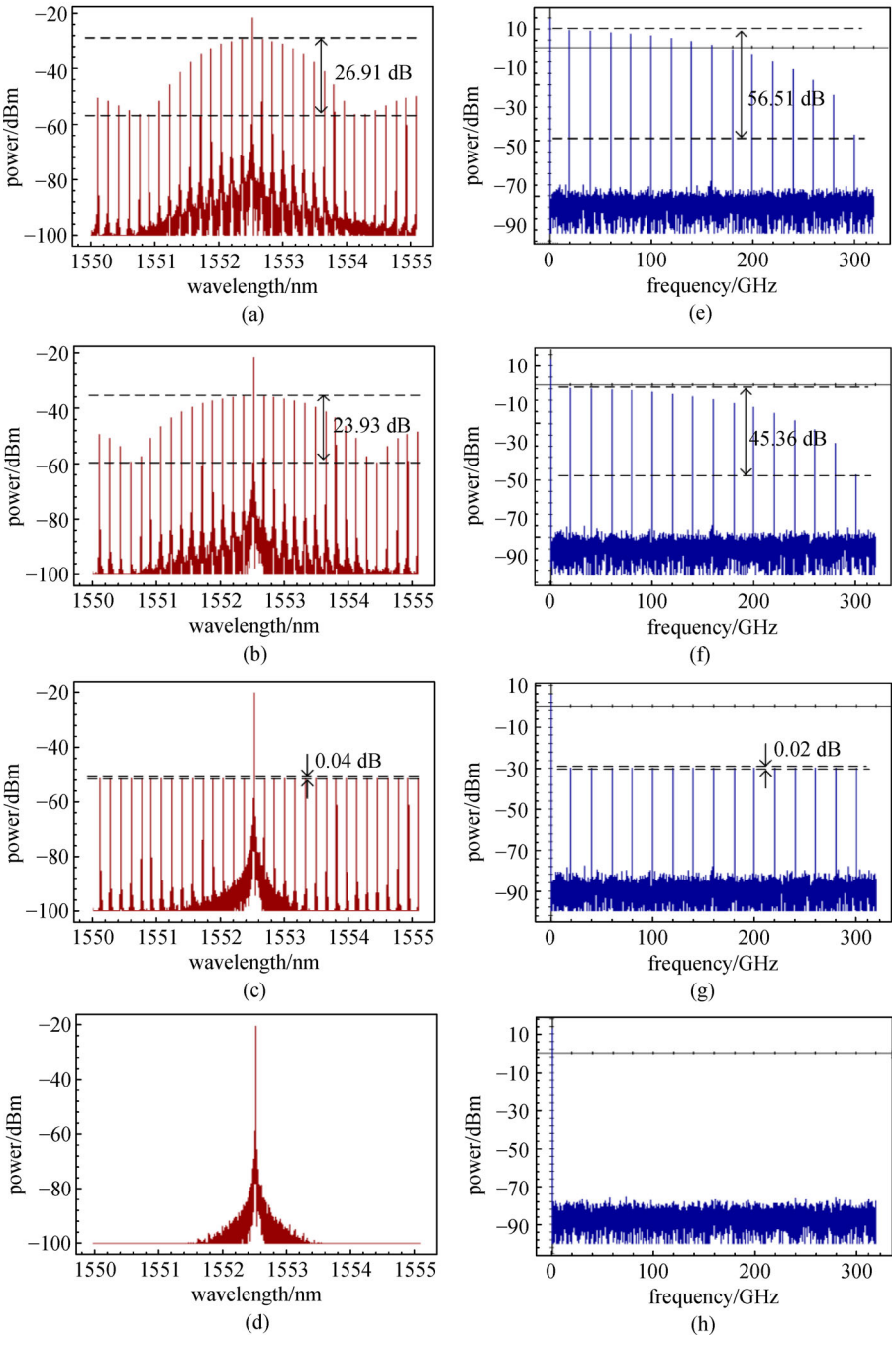


**Fig. 3** Output optical spectra from MQW-EAM (a)–(d) and the corresponding output electrical spectra from PD (e)–(h) with the $V_b$ to be: (a) and (e) 6.52, (b) and (f) 6.72, (c) and (g) 6.92, (d) and (h) 7.12 V, respectively

with the increase of $V_b$. Besides, the corresponding power variation is 1.41, 0.14, 0.02 and 0.02 dB, which is improved with the increase of $V_b$. So, with the fluctuation of the $V_b$ near the critical state, the average power of MFC and the power variation change a little. Therefore, the voltage fluctuation within 0.02 V near the critical state has a slight effect on the performance of the MFC. Currently, the voltage accuracy of 0.01V on MQW-EAM can be achieved.

### 4.5 Effects of the linewidth of TLD

Figure 7 shows the spectra of the MFCs when the linewidth of TLD is 1, 10, 100 MHz and 1 GHz. We can see that the corresponding average power is almost unchanged. The power variation of each case is maintained at 0.02 dB. This main reason is that when beatings occurs, the phase of the two optical signals needs to satisfy a certain relationship to generate microwave signals, while

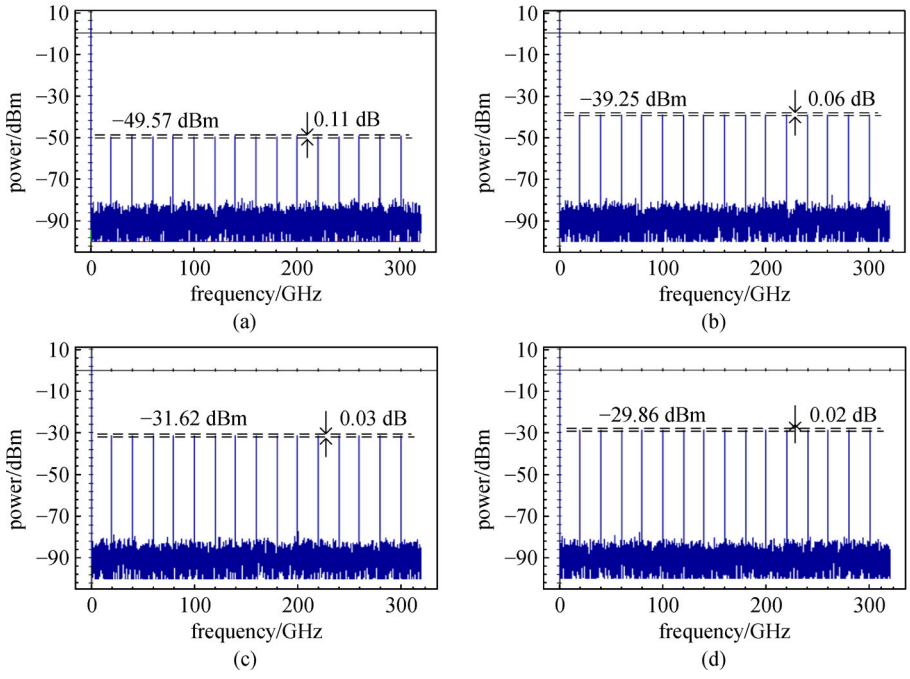


**Fig. 4** Output electrical spectra from PD with the voltage of the RF signal $V_{RF}$ to be (a) 1, (b) 4, (c) 7 and (d) 10 V, and the corresponding $V_b$ to be 2.49, 3.97, 5.43 and 6.92 V respectively

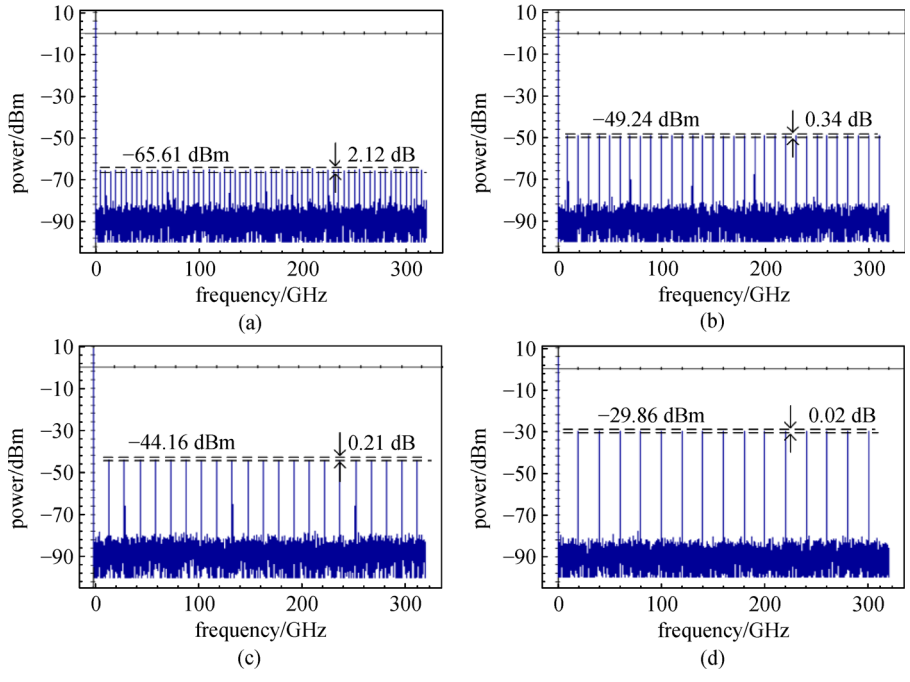


**Fig. 5** Output electrical spectra from PD with the frequency of the RF signal to be (a) 5, (b) 10, (c) 15 and (d) 20 GHz, and the corresponding $V_b$ to be 6.99, 6.98, 6.97 and 6.92 V respectively

other light whose phases do not satisfy the requirements will not beat. So different linewidth of light will not affect the MFC generated. Therefore, the MFC is independent on the linewidth of TLD.

### 4.6 Effects of the gain of EDFA

Figure 8 shows the spectra of the MFCs when the small-signal gain of the EDFA is 25, 30, 35 and 40 dB. As can be

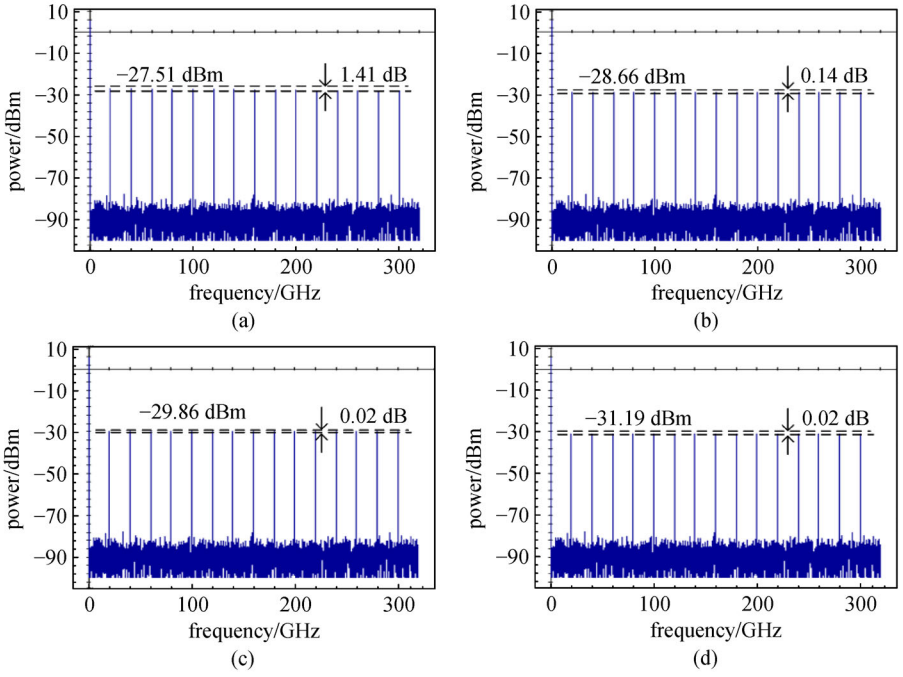


**Fig. 6** Output electrical spectra from PD with the $V_b$ to be (a) 6.90, (b) 6.91, (c) 6.92 and (d) 6.93 V respectively

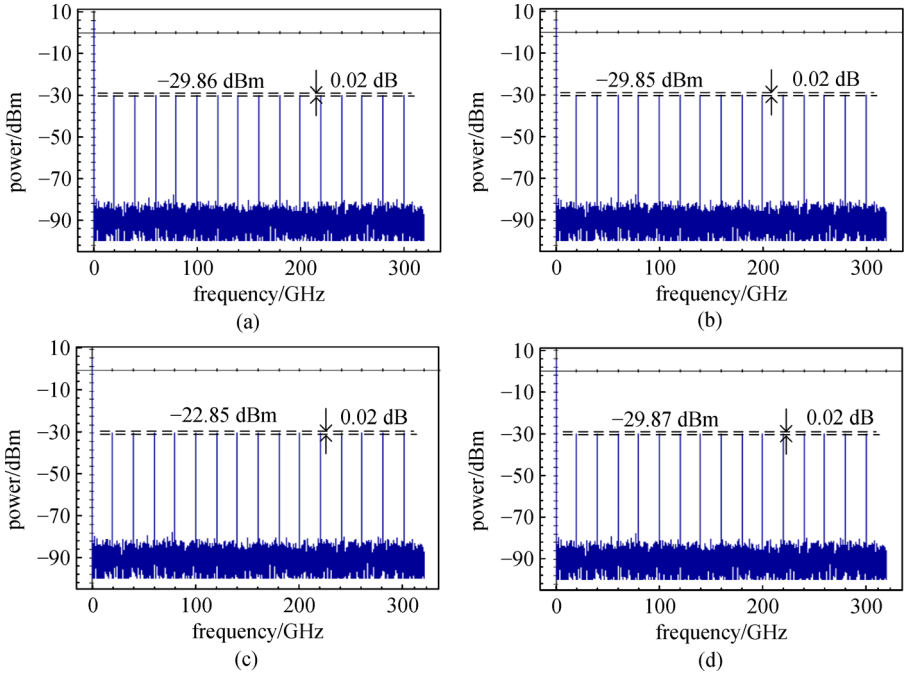


**Fig. 7** Output electrical spectra from PD with the linewidth of TLD to be (a) 1, (b) 10, (c) 100 MHz and (d) 1 GHz, respectively

seen that the corresponding average power becomes higher with the increase of the gain. Besides, the power variation is improved along with the small-signal gain becoming larger. This is mainly because small-signal gain is the key parameter to measure the amplification effect of EDFA on optical signal. The larger it is, the stronger the amplification effect on the input optical signal is, and the greater the power of the amplified output optical signal is. Deservedly, the average power of MFC generated by beatings is larger. So the performance of the MFC can be improved by increasing the small-signal gain of the EDFA.

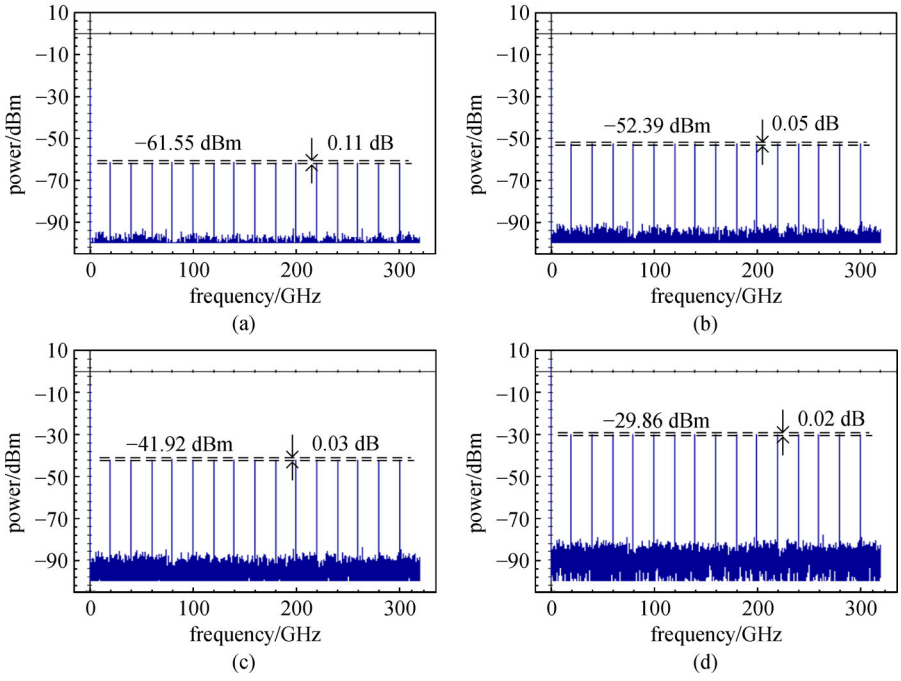


**Fig. 8** Output electrical spectra from PD with the gain of EDFA to be (a) 25, (b) 30, (c) 35 and (d) 40 dB, respectively

### 4.7 Effects of the responsivity of PD

Figure 9 shows the spectra of the MFCs when the responsivity of PD is 0.4, 0.7, 1.0 and 1.3 A/W. As can be seen that the corresponding average power is −37.81, −32.95, −29.86 and −27.57 dBm, and the corresponding power variation is 0.03, 0.03, 0.02, and 0.02 dB. Therefore, with the increase of the responsivity, the average power increases and the power variation maintains about 0.02 dB. The main reason is that responsivity is an important parameter of energy conversion efficiency of PD, which is the ratio of the average output current of the detector to the

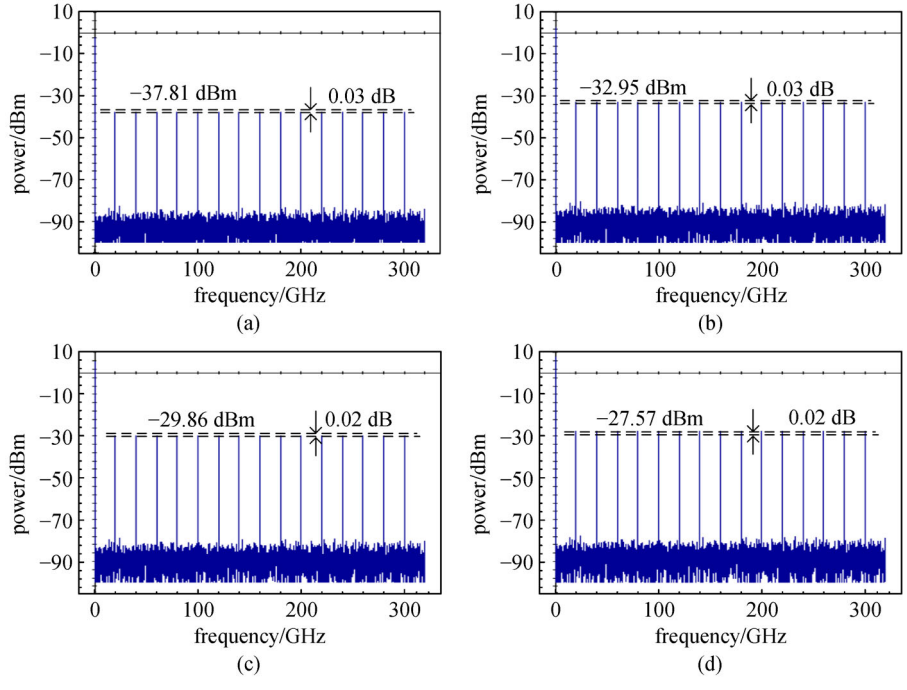


**Fig. 9** Output electrical spectra from PD with the responsivity of the PD to be (a) 0.4, 0.7, 1.0 and 1.3 A/W, respectively

average input light power. The larger the responsivity is, the higher the photoelectric conversion efficiency is, the larger the current converted from the same light power. So the performance of the scheme will be better by using PD with higher responsivity.

## 5 Conclusion

We have proposed a novel scheme to generate an ultra-flat broadband MFC based on OFC with a MQW-EAM in critical state. This scheme has the advantages of simple structure and easy adjustability. The simulation is performed using the software Optisystem and the effects of some parameters on the MFCs are analyzed. The results show that, an ultra-flat broadband MFC can be generated by adjusting the bias voltage of the MQW-EAM and the voltage of the RF signal to make the MQW-EAM in critical state. The MFC has 300-GHz effective bandwidth with the power variation of 0.02 dB and 15 comb lines. The comb spacing of MFC can be adjusted from 5 to 20 GHz by changing RF signal's frequency and the performance of the MFC can be improved by reasonably adjusting the voltage of the RF, the gain of the EDFA and the responsivity of the PD. Besides, The MFC is almost independent on the linewidth of the TLD.

**Acknowledgements** Related studies were supported by the National Natural Science Foundation of China (Grant No. 61275067).

## References

1. Hunter D B, Minasian R A. Photonic signal processing of microwave signals using an active-fiber Bragg-grating-pair structure. IEEE Transactions on Microwave Theory & Techniques, 1997, 45(8): 1463–1466
2. Yokoyama S, Nakamura R, Nose M, Araki T, Yasui T. Terahertz spectrum analyzer based on a terahertz frequency comb. Optics Express, 2008, 16(17): 13052–13061
3. Doloca N R, Meiners-Hagen K, Wedde M, Pollinger F, Abou-Zeid A. Absolute distance measurement system using a femtosecond laser as a modulator. Measurement Science & Technology, 2010, 21(11): 115302
4. Woo K, Liu Y, Nam E, Ham D. Fast-lock hybrid PLL combining fractional-*N* and integer-*N* modes of differing bandwidths. IEEE Journal of Solid-State Circuits, 2008, 43(2): 379–389
5. Ma H, Tang X, Wu T, Cao Z. New method to design a low-phase-noise millimeter-wave PLL frequency synthesizer. Microwave and Optical Technology Letters, 2006, 48(6): 1194–1197
6. Li Q, Jiang W, Xu Y, Nian F. Analysis and design of wide-band comb generator based on SRD. In: Proceedings of International Conference on Microwave and Millimeter Wave Technology (ICMMT). Shenzhen: IEEE, 2012, 1–3
7. Madani K, Aitchison C S A. 20 GHz microwave sampler. IEEE Transactions on Microwave Theory and Techniques, 1992, 40(10): 1960–1963
8. Hagmann M J, Efimov A, Taylor A J, Yarotski D A. Microwave frequency-comb generation in a tunneling junction by intermode mixing of ultrafast laser pulses. Applied Physics Letters, 2011, 99(1): 011112
9. Hagmann M J, Taylor A J, Yarotski D A. Observation of 200th harmonic with fractional linewidth of $10^{-10}$ in a microwave frequency comb generated in a tunneling junction. Applied Physics Letters, 2012, 101(24): 241102
10. Chan S C, Xia G Q, Liu J M. Optical generation of a precise microwave frequency comb by harmonic frequency locking. Optics Letters, 2007, 32(13): 1917–1919
11. Juan Y S, Lin F Y. Ultra broadband microwave frequency combs generated by an optical pulse-injected semiconductor laser. Optics Express, 2009, 17(21): 18596–18605
12. Fan L, Xia G Q, Tang X, Deng T, Chen J J, Lin X D, Li Y N, Wu Z M. Tunable ultra-broadband microwave frequency combs generation based on a current modulated semiconductor laser under optical injection. IEEE Access, 2017, 5: 17764–17771
13. Deng Z, Yao J. Photonic generation of microwave signal using a rational harmonic mode-locked fiber ring laser. IEEE Transactions on Microwave Theory and Techniques, 2006, 54(2): 763–767
14. Hagmann M J, Henage T E, Azad A K, Yarotski D A, Taylor A J. Frequency comb from 500 Hz to 2 THz by optical rectification in zinc telluride. Electronics Letters, 2013, 49(23): 1459–1460
15. Gao S, Gao Y, He S. Photonic generation of tunable multi-frequency microwave source. Electronics Letters, 2010, 46(3): 236–248
16. Wu D, Xue X, Li S, Zheng X, Xiao X, Zha Y, Zhou B. Photonic generation of multi-frequency phase-coded microwave signal based on a dual-output Mach-Zehnder modulator and balanced detection. Optics Express, 2017, 25(13): 14516–14523
17. Cai C, Liu X, Zhang M D, Sun X H. Experimental research on dispersion characteristics of strip InP/InGaAsP-MQW-EAM. Journal of Optoelectronics Laser, 2008, 19(4): 434–438
18. Li W L, Yu C Y, Fei B, Gao D, Gu J, Zhu W Z. Single electro absorption modulator based generation of super flat dual optical frequency combs. Study on Optical Communications, 2015(4): 42–45
19. Mitomi O, Nojima S, Kotaka I, Wakita K, Kawano K, Naganuma M. Chirping characteristics and frequency response of MQW optical intensity modulator. Journal of Lightwave Technology, 1992, 10(1): 71–77
20. Tang J X. Optical beat frequency and interference phenomenon. College Physics, 1990, 1(1): 10–12

**Cong Shen** is currently a third-year postgraduate student of Nanjing University of Posts and Telecommunications majoring in industrial engineering. His research direction is optical communication. His academic area is optical fiber communication and optical waveguide technology. His research consists of five parts, namely, research problems and significance, theoretical bases of the study, methodology, results, and innovation and limitations of the study.

**Peili Li** received the B.S. degree in physics from Wuhan University, Wuhan, China, in 1996, the M.Sc. degree in physical electronics from the Institute of Laser Technology and Engineering, and the Ph.D. degree from the Department of Optoelectronics Engineering in Huazhong University of Science and Technology, Wuhan, China, in 2000. She worked toward Postdoctor in Wuhan National Laboratory for Optoelectronics in 2007. Now she is working in Nanjing University of Posts and Telecommunications. Her research interests are optoelectronic devices, fiber communication systems, and numerical modeling and simulation of semiconductor optical devices.